



HAL
open science

ORAI3 silencing alters cell proliferation and promotes mitotic catastrophe and apoptosis in pancreatic adenocarcinoma.

Nathalie Ziental Gelus, Fabien Vanden Abeele, Charlotte Dubois, Kateryna Kondratska, Artem Kondratskyi, Angela Morabito, Lina Mesilmany, Valerio Farfariello, Robert-Alain Toillon, Nathalie Ziental Gelus, et al.

► To cite this version:

Nathalie Ziental Gelus, Fabien Vanden Abeele, Charlotte Dubois, Kateryna Kondratska, Artem Kondratskyi, et al.. ORAI3 silencing alters cell proliferation and promotes mitotic catastrophe and apoptosis in pancreatic adenocarcinoma.. *Biochimica et Biophysica Acta - Molecular Cell Research*, 2021, 1868 (7), pp.119023. 10.1016/j.bbamcr.2021.119023 . inserm-03237118

HAL Id: inserm-03237118

<https://inserm.hal.science/inserm-03237118>

Submitted on 26 May 2021

HAL is a multi-disciplinary open access archive for the deposit and dissemination of scientific research documents, whether they are published or not. The documents may come from teaching and research institutions in France or abroad, or from public or private research centers.

L'archive ouverte pluridisciplinaire **HAL**, est destinée au dépôt et à la diffusion de documents scientifiques de niveau recherche, publiés ou non, émanant des établissements d'enseignement et de recherche français ou étrangers, des laboratoires publics ou privés.

Title: ORAI3 silencing alters cell proliferation and promotes mitotic catastrophe and apoptosis in pancreatic adenocarcinoma.

Running title: Involvement of ORAI3 in PDAC

Authors : Charlotte DUBOIS^{1*}, Kateryna Kondratska^{1*}, Artem Kondratskyi¹, Angela MORABITO^{1,2}, Lina MESILMANY¹, Valerio FARFARIELLO¹, Robert-Alain TOILLON³, Nathalie ZIENTAL GELUS¹, Emilie LAURENGE¹, Fabien VANDEN ABEELE¹, Loic LEMONNIER^{1#}, Natalia PREVARSKAYA^{1#}

¹Univ. Lille, Inserm, U1003 - PHYCEL - Physiologie Cellulaire, 59000 Lille, France.

² actual address: University of Lille, CNRS, Inserm, CHU Lille, Institut Pasteur de Lille, UMR9020 - UMR-S 1277 - Canther - Cancer Heterogeneity, Plasticity and Resistance to Therapies, Lille, France.

³ Univ. Lille, Inserm, U908, 59000 Lille, France.

* co-first author

co-senior author

Abstract

Changes in cytosolic free Ca²⁺ concentration play a central role in many fundamental cellular processes including muscle contraction, neurotransmission, cell proliferation, differentiation, gene transcription and cell death. Many of these processes are known to be regulated by Store-Operated Calcium channels (SOCs), among which ORAI1 is the most studied in cancer cells, leaving the role of other ORAI channels yet inadequately addressed. Here we demonstrate that ORAI3 channels are expressed in both normal (HPDE) and pancreatic ductal adenocarcinoma (PDAC) cell lines,

where they form functional channels, their knockdown affecting Store Operated Calcium Entry (SOCE). More specifically, ORAI3 silencing increased SOCE in PDAC cell lines, while decreasing SOCE in normal pancreatic cell line. We also show the role of ORAI3 in proliferation, cell cycle, viability, mitotic catastrophe and cell death. Finally, we demonstrate that ORAI3 silencing impairs pancreatic tumor growth and induces cell death *in vivo*, suggesting that ORAI3 could represent a potential therapeutic target in PDAC treatment.

Highlights:

- ORAI3 is expressed in PDAC and normal epithelial pancreatic cell lines
- ORAI3 silencing increases SOCE in PDAC while decreasing it in normal cells
- ORAI3 silencing impairs MiaPaCa2 survival and mediates mitotic catastrophe & cell death

Keywords: calcium channels; ORAI3; mitotic catastrophe; apoptosis; PDAC

1. Introduction

According to GLOBOCAN 2018, Pancreatic ductal adenocarcinoma (PDAC) is the seventh leading cause of cancer-related death in the world with an estimated 432,242 deaths occurring in 2018 [1]. Pancreatic cancer has a 5-year survival rate of only 9%, which is a consequence of an asymptomatic course of the disease till the late incurable stages, as well as of a high resistance of this cancer to existing chemotherapies and radiotherapies [2,3].

Pancreatic cancer chemoresistance is multifactorial as a result of the interaction between pancreatic cancer cells, cancer stem cells, and tumor microenvironment . Mechanisms contributing to therapeutic escape observed in PDAC include, among others, gene mutations, aberrant gene expression, and deregulation of many signaling pathways. Thus, understanding the physiology of pancreatic cancer cells is of great importance as it can reveal novel approaches for treating this cancer.

Cancer is generally caused by defects in the mechanisms controlling cell proliferation and cell death. Calcium ions are central to these phenomena and thus are inextricably linked to cancer initiation (regulation of autophagy, senescence etc.) and progression (regulation of proliferation, migration and apoptosis resistance) [4]. The malignant transformation of a cell is generally associated with a major rearrangement of the Ca^{2+} signaling toolkit, leading to enhanced proliferation, invasion, apoptosis resistance and overall cancer progression. However, it should be noted that calcium signaling can also contribute to the suppression of tumorigenesis at both early and late stages by regulating such important processes as autophagy, senescence and apoptosis [4,5].

Store-operated calcium channels (SOCs) represent one of the major calcium-entry pathway in non-excitabile cells and are widely distributed in various cell types. SOCs are plasma membrane ion channels activated in response to the Endoplasmic Reticulum (ER) Ca^{2+} stores depletion and thereby provide Ca^{2+} for ER stores refilling as well as for signaling purposes [6,7]. The major molecular components of SOC are stromal interaction molecule 1 (STIM1) and ORAI1 proteins. ORAI1 constitutes a plasma membrane calcium channel and STIM1 represents a mostly ER-localized single-transmembrane domain protein, functioning as an ER calcium sensor. Following ER Ca^{2+} stores depletion, STIM1 translocates to ER regions near the plasma membrane, where it interacts with and activates ORAI1 channel, thereby mediating store-operated calcium entry (SOCE) [8,9]. Although ORAI channels and their regulator STIM1 were originally identified and described as key components of store-operated highly calcium-selective SOC channels, it is now clear that these proteins are equally essential components of the agonist-activated, store-independent calcium entry pathway mediated by the arachidonic acid-regulated calcium-selective (ARC) channel. ARC channels display biophysical properties that closely resemble those of CRAC channels but, whereas the latter is formed exclusively by ORAI1 subunits, the ARC channel is formed by a combination of ORAI1 and ORAI3 subunits. Orai3 is a highly conserved paralogue of Orai1 [10]. Indeed ORAI1 and ORAI3 proteins show a high degree (~82%) of conservation and can associate with each other to form an heteromeric channel sharing the same high selectivity for calcium as ORAI1 homomeric channel in physiological conditions [10]. Similar to ORAI1, ORAI3 appears to have a broad expression pattern [10–12], but in contrast to ORAI1, ORAI3 is an exclusively mammalian protein. In estrogen receptor-positive breast cancer cells ORAI3 (but not ORAI1) has been shown to

mediate SOCE [13]. In prostate cancer cells, we previously showed that ORAI3 overexpression leads to the formation of more ORAI1/3 heteromers promoting cell proliferation (via arachidonic acid-mediated Ca^{2+} entry) while decreasing the formation of homomeric ORAI1 (SOC) channels [14]. In non small cell lung cancer it has been described that pharmacological inhibition or knockdown of Orai3 reduces SOCE and cell proliferation via cell cycle arrest [15]. Moreover, ORAI3 increased expression was also reported to mediate decreased SOCE sensitivity to reactive oxygen species (ROS) in human T helper (Th) lymphocytes and siRNA against ORAI3 rendered effector Th cells more redox-sensitive. [16].

We have previously shown that ORAI1 and STIM1 are expressed in PDAC where they mediate SOC and participate to chemotherapeutic resistance in PDAC [17]. The role of ORAI3 in these processes remains however elusive to this date. Here we demonstrate that ORAI3 channels (1) are overexpressed in PDAC samples from patients (2) are overexpressed in PDAC cell lines compared to normal human pancreatic duct epithelial (HPDE) H6C7 cell line and (3) that their knockdown affected SOCE. More specifically, we show that ORAI3 silencing increases SOCE in PDAC cell lines, while decreasing it in HPDE. We also demonstrate the role of ORAI3 in proliferation, cell cycle and viability in MiaPaCa2 cells. We further demonstrate that silencing of ORAI3 impairs pancreatic tumor growth *in vivo* via apoptosis induction, suggesting that ORAI3 could represent a potential therapeutic target in PDAC treatment.

2. Material and methods

2.1 Cell culture and transfection

Pancreatic adenocarcinoma cell line Panc1 from the American Type Culture Collection (ATCC) was cultured in Dulbecco's Modified Eagle Medium DMEM+GlutaMAX (31966, Invitrogen, Life Technologies Inc.) supplemented with 10% Foetal Calf Serum (FCS, PAA Gold). Pancreatic adenocarcinoma cell lines ASPC1 and BxPC3 obtained from the ATCC were cultured in RPMI 1640 medium (31870, Gibco-Life Technologies) supplemented with 5 mM L-glutamine (25030, Gibco) and 10% FCS (PAA Gold). Pancreatic adenocarcinoma cell line MiaPaCa2 (ATCC) was cultured in DMEM/F12 medium (31330, Gibco-Life Technologies) supplemented with 2,5% Horse Serum (S 9135, Biochrom) and 10% FCS (PAA Gold). Pancreatic adenocarcinoma cell line Capan1 (ATCC) was cultured in IMDM medium (SH 30229.01 HyClone, ThermoScientific) supplemented with 20% FCS (PAA Gold). Immortalized human pancreatic ductal epithelial cells H6C7 were kindly provided from Dr. Ming-Sound Tsao (University Health Network, Toronto, ON, Canada) and cultured in KBM medium (CC-3101, Lonza) supplemented with KGM SingleQuots (CC-4131, Lonza).

Cells were transfected with 40 nM of siRNA against ORAI3 or luciferase here after siCT (Eurogentec, France, or Dharmacon Inc., Fremont, CA, USA) using Hyperfect transfection reagent (Qiagen Inc.), following manufacturer's instructions. siRNA sequences were:

siCT 5'-CUUACGCCUGAGUACUUCGA(dTdT)-3';

siOrai3 5'-UUGAAGCUGUGAGCAACAUA (dTdT)-3'

2.2 Antibodies and reagents

Thapsigargin (TG) (1138) was obtained from Tocris. Mouse anti-PCNA (PC10) was ordered from Santa Cruz (sc-56). Rabbit polyclonal anti-PARP and PARP cleaved

antibody were obtained from Cell Signaling (Cell Signaling 9542s). Mouse anti- β Actin (A5441) was obtained from Sigma and Hoechst 33258 from Invitrogen.

2.3 Calcium imaging

Pancreatic cancer cells were grown on glass coverslips prior to carrying out calcium imaging experiments. Ratiometric dye Fura-2/AM (F1221, Invitrogen) was used as a Ca^{2+} indicator. Cells were loaded with 2 μM Fura-2/AM for 45 min at 37°C and 5% CO_2 in corresponding culture medium and subsequently washed three times with external solution containing (in mM): 140 NaCl, 5KCl, 1 MgCl₂, 2 CaCl₂, 5 Glucose, 10 HEPES (pH 7.4 adjusted with NaOH). Coverslips were then transferred in a perfusion chamber on a microscope stage (Nikon Eclipse Ti). Fluorescence was alternatively excited at 340 and 380 nm with a monochromator (Polychrome IV, TILL Photonics GmbH) and captured at 510 nm by a CCD camera (QImaging). Acquisition and analysis was performed with MetaFluor 7.7.5.0 software (Molecular Devices Corp.). Analysis of the ER calcium content has been calculated using the area under the curve of the calcium changes after thapsigargin administration in the absence of extracellular Ca^{2+} to estimate endoplasmic reticulum calcium content as described in [18]

2.4 RT-PCR

Total RNA was extracted using TRI reagent (Sigma) and treated with DNase (Ambion). cDNA was synthesized by reverse transcription. qRT-PCR was performed in a real-time thermal cycler Cfx C1000 (Biorad) using EvaGreen Supermix (Biorad). Primers are listed in Table 1.

Table 1. List of primers used for qPCR

N	Name	Forward (5'-...-3')	Backward (5'-...-3')
1	hGAPDH	TTCGTCATGGCTGTGAACCA	CAGTGATGCGCATGGACTGT
2	hHPRT	GGCGTCGTGATTAGTGATGAT	CGAGCAAGACGTTTCAGTCCT
3	hOrai3	GACCGCTACAAGCAGGAACT	ATCCTTCAACTGAGGCCAGC

2.5 Apoptosis assays

The level of apoptosis was determined by Hoechst and TUNEL staining *in vitro* and *in vivo*. Cells were grown on 6-well plates and transfected with siCT or siORAI3. At the end of the treatments, both floating and attached cells were collected by trypsinization, centrifuged and resuspended in 1 ml of phosphate-buffered saline (PBS). Following cytopspining, cells were fixed with ice-cold methanol for 10 min, washed with PBS and stained with 5 µg/ml Hoescht for 10 min at room temperature or with *in situ* TUNEL (TMR red Roche). Briefly, according to manufacturer's protocols, cells were fixed in 4% PFA/PBS (15 min, Room Temperature (RT)) and permeabilized with 0,25% Triton 100X /PBS (20 min, RT). After TdT reaction (60 min, 37°C), cells were stained with Hoechst/PBS (1/500) for 15min at RT. For formalin-fixed and paraffin-embedded tissues, tumor slices (6µm) were incubated with PBS-Gelatin at 37°C in a humidified chamber. After TUNEL staining reaction (60 min, 37°C), cells were washed twice with PBS-G. Finally, cells were stained with Hoechst/PBS (1/500) for 15 min at RT. Staining was visualized on Zeiss Axio Imager A1 fluorescence microscope and with LSM 700 confocal imaging system. For Hoeschst staining, percentage of apoptotic cells (with condensed/fragmented nuclei) was determined by counting at least 500 cells in random fields.

2.6 Western blotting

Cells were washed with cold PBS and lysed in ice-cold buffer containing: 1% Triton X-100, 150 mM NaCl, 5 mM EDTA, 1% Sodium deoxycholate, 10 mM PO₄Na₂/K buffer, a protease inhibitor cocktail (Sigma-Aldrich) and a phosphatase inhibitor cocktail PhosSTOP (Roche). Lysates were centrifuged at 15,000×g at 4°C for 15 minutes to remove cell debris and supernatant protein concentration was determined by the BCA protein assay kit (Pierce Biotechnology). 30 µg of total protein were subjected to SDS-PAGE followed by transfer to PVDF or nitrocellulose membranes using the Trans-Blot® SD semi-dry transfer cell (Bio-Rad). The membranes were blocked in a 5% fat-free milk containing TNT buffer (Tris-HCl, pH 7.5, 140 mM NaCl, and 0.05% Tween 20) for 1h at room temperature (RT). The membranes were next incubated overnight at 4°C with primary antibodies, and then for 1 h at RT with secondary antibodies conjugated to horseradish peroxidase. After washing, the membranes were processed for chemiluminescence detection using Luminata Western HRP substrate (Milipore). Image J software was employed for quantitative analysis.

2.7 Cell viability assay

Cells were seeded at 10,000 cells/well on 96-well plates in normal medium. The cells were treated either with siRNA for 48h in complete media. Cell viability was monitored using the CellTiter 96 Aqueous One Solution cell proliferation assay (Promega), on the basis of the cellular conversion of the colorimetric reagent MTS [3,4-(5-dimethylthiazol-2-yl)-5-(3-carboxymethoxyphenyl)-2-(4-sulfophenyl)-2H-tetrazolium salt] into soluble formazan by dehydrogenase enzymes found only in metabolically active cells. Following treatment cells were incubated with reagent solution and absorbance was recorded at 490 nm wavelength using an ELISA plate reader (Molecular Devices).

2.8 Clonogenic assay

The MiaPaCa2 cells were seeded in a 6-well plate in normal medium (500 cells per well) and transfected with siCT or siORAI3. The next day the medium was changed and cells were left to recover for 10 days. Cells were then washed with PBS and fixed with methanol:acetic acid (3:1) for 5 min at room temperature. Cells were then stained with 0.5% crystal violet (in methanol) for 2h, washed with tap water and dried. Cell colonies were then photographed and counted.

2.9 Cell cycle analysis

MiaPaCa2 cells were seeded in 6-cm dishes in normal medium and transfected with either siCT or siORAI3. After 96 hours, cells were collected by trypsinization, centrifuged and washed with PBS and fixed overnight with 70% ice-cold ethanol at – 20 °C. Fixed cells were treated with RNase A (100 µg/ml) for 15 min at room temperature, and stained with a PBS-based solution containing Propidium Iodide (50 µg/ml). Cell cycle was analyzed with Cyan LX9 cytometer (Beckman Coulter, France) and data were processed with Summit 4.5 software (Beckmann Coulter, France).

2.10 Confocal microscopy

Cell images were obtained using confocal laser scanning microscope (LSM 700, Carl Zeiss MicroImaging GmbH) with a Plan Apochromat 40x/1.3 numerical aperture oil immersion objective. Images were analyzed with Zeiss LSM Image Browser software or Fiji [19] and prepared for publication in Adobe Photoshop.

2.11 Animal experiments

Studies involving animals, including housing and care, method of euthanasia, and experimental protocols, were conducted in accordance with local animal ethical committee guidelines (C59-00913; protocol CEEA 202012) of the University of Lille. MiaPaCa2 cells were plated in T75 flasks. After reaching 80% confluency, cells were washed with PBS, trypsinized, washed and centrifuged (1000 rpm/5 min). Two millions cells were resuspended in 50% (v:v) Matrigel (BD Biosciences, 100 μ L) and were then injected subcutaneously into 6- to 8-week-old female nude mice. After tumor formation, mice were injected i.p. with siRNA diluted in sterile PBS on a daily basis. After a week (day 1) tumors were measured every 4 days and tumor volume was calculated as $\text{volume} = (\text{length} \times \text{width}^2)/2$.

2.12 Bioinformatic analysis of public PDAC data set

ORAI1 and ORAI3 gene expression have been determined using Gene Expression Omnibus (GEO). Data were extracted and analysed using R and BioConductor package to convert probe IDs during the microarray analysis workflow as described. [20].

2.13 Data analysis

Data were analyzed using Origin 7.0 (Microcal Software). Statistical analysis was performed using Student's t-test, and $p < 0.05$ was considered as significant. Asterisks denote: * - $p < 0.05$, ** - $p < 0.01$ and *** - $p < 0.001$.

3. Results

3.1 ORAI3 is over-expressed in PDAC tumors compared to normal tissue.

We analyzed microarray data sets of human PDAC available in the public domain, for ORAI1 and ORAI3 gene expression. Pairs of normal and tumor tissue samples

were obtained at the time of surgery from resected pancreas of 36 pancreatic cancer patients (GEO accession: GSE15471)[21]. We found that ORAI1 is decreased in tumor tissue (normal tissue $\text{Log}(2)=6.82$ vs $\text{Log}(2)=6.54$ for tumor tissue $p = 0.004$) and that ORAI3 expression is increased in tumor tissue compared to adjacent normal tissue (normal tissue $\text{Log}(2) = 8.08$ vs $\text{Log}(2)= 8.37$ for tumor tissue $p = 0.000463$) (Figure 1A).

3.2 ORAI3 is differentially expressed in PDAC and H6C7 cell lines.

We then analyzed the expression of ORAI3 at the mRNA level using qRT-PCR technique on several PDAC models (BxPC3, Capan1, MiaPaCa2 and Panc1), a model derived from a metastatic ascite (ASPC1) and an immortalized normal human pancreatic duct epithelial (HPDE) cell line (H6C7). We found that ORAI3 is expressed in all cell lines tested. The level of expression is higher in PDAC cells compared to HPDE cells, increasing from a 2 to 7 fold change depending on cell lines (Figure 1B).

3.3 Involvement of ORAI3 in SOCE in PDAC and HPDE cell lines.

Our next goal was to investigate if ORAI3 contributes to SOCE in PDAC and H6C7 cells. H6C7, AsPC1, BxPC3, MiaPaCa2, Capan1 and Panc1 cell lines were transfected with siCT or siORAI3 (40nM/48h). Cells were then loaded with Fura2/AM dye and subjected to calcium imaging experiments. We checked whether siRNA-mediated knockdown of ORAI3 influences cytosolic calcium levels in PDAC and H6C7 cells using acute thapsigargin (TG, 1 μ M) treatment. Experimental protocol was as follows: experiments start in calcium free extracellular saline (HBSS) condition; addition of TG at 200s reveals the amount of internal calcium stores (ER stores); subsequent addition of 2mM Ca^{2+} at 500s to the medium initiates a calcium influx via

SOC channels. Silencing of ORAI3 in H6C7 cells resulted in slightly decreased SOCE (Figure 2A & 2B). Surprisingly, when this assay was performed on siORAI3-transfected PDAC cells (AsPC1, BxPC3, MiaPaCa2, Capan1 and Panc1 cells), calcium entry was significantly increased (Figure 2C-L). We also quantified calcium release from the ER following SERCA pump inhibition (TG in calcium free solution, 200-500s), and showed that ORAI3 silencing increases ER calcium release in pancreatic cell lines (except for BxPC3 cells even if we do observe an increase in SOCE, see Figure 2C & D) and decreases ER calcium release in normal pancreatic cells (HPDE) (Fig S1 A-F).

Alternatively, ER calcium stores were depleted by a preincubation in 0 Ca^{2+} extracellular solution for 30 min. SOCE was stimulated by the addition of 10mM Ca^{2+} to the extracellular media. This protocol was performed on MiaPaCa2, Capan1 and Panc1 cell lines. We again observed in siORAI3-transfected cells a significant increase of SOCE amplitude compared to control (siCT, Figure 3A-C). Efficiency of siRNAs transfection at 48h was confirmed using qRT-PCR (Figure S2 G-K).

As mentioned in the introduction, ORAI3 is known to be able to interact with ORAI1 to form the ARC channel activated by arachidonic acid (AA). We thus performed calcium imaging on normal HPDE cells and cancerous MiaPaCa2 exposed to AA. As shown in Figure 3D, normal cells in 2mM calcium HBSS do not respond to AA (8 μM) contrary to MiaPaCa2 cells (Figure 3D). Moreover, in cells pre-treated with AA (30min/ 8 μM), TG-induced SOCE is drastically decreased. These results suggest that the AA-induced recruitment of ORAI1 to form ARC channels with ORAI3 could impede the formation of SOC channels and thus limit SOCE in PDAC cells.

It has been described that SOC inhibitors induce proliferation defects in pancreatic cell lines including Panc1 and MiaPaCa2 [22,23]. We have selected Synta66, which does not affect STIM1/ORAI1 interaction but directly blocks ORAI1 pore, to evaluate its effect on cell proliferation. We observed that Synta66 (5 μ M/DMSO) decreases MiaPaCa2 proliferation by 20% after a 48h treatment compared to control cells (treated with DMSO) (Fig S2 A). We then performed experiments combining siRNA treatments with SOC inhibition, and we observed the same effect of Synta66 on cells treated with siCT or siORAI3. Proliferation was measured at day 3, a time point where we see the effects of ORAI3 silencing. As presented in the corresponding MTS assay, we do not observe more inhibition of proliferation in cells silenced for ORAI3 than in cells treated with siCT + Synta66 (Fig S2 B). These results strongly support our previous conclusions that ORAI1/ORAI3 heteromers control PDAC cells proliferation, with little to no impact of ORAI1 homomers.

3.4 ORAI3 influences PDAC cells proliferation and morphological changes.

Our next goal was to examine how ORAI3 silencing affects PDAC cells proliferation. Panc1, Capan1 and MiaPaCa2 cells were plated on 96-well plates, and were either left untransfected (CT) or transfected with siCT or siORAI3 for 48h. Cell proliferation was monitored 48h later (i.e. 96h after beginning the experiment) using CellTiter 96 Aqueous One Solution cell proliferation assay (MTS assay). ORAI3 silencing significantly reduced proliferation rate in the three cell lines tested, suggesting that ORAI3 regulates PDAC cells proliferation (Figure 4A, 4B & 4C).

Interestingly, starting from day 2 after siORAI3 transfection, we observed remarkable changes in PDAC cells morphology. Observation under light microscopy revealed a significant increase in cell size, an unusual cell shape, as well as cell flattening for

siORAI3-transfected MiaPaCa2, BxPC3 and Panc1 cells compared to siCT-transfected cells (Figure 4D).

For subsequent experiments, we focused on the role of ORAI3 in MiaPaCa2 cells, as ORAI3 silencing in these cells induced the most significant changes in both morphology and cell number.

3.5 ORAI3 controls cell proliferation and cell cycle progression in MiaPaCa2.

First, to confirm the role of ORAI3 in MiaPaCa2 proliferation, we performed manual cell counting as well as immunodetection of widely used proliferation marker PCNA (proliferating cell nuclear antigen). Consistent with our previous results, ORAI3 silencing reduced the number of MiaPaCa2 cells (Figure 4E) and decreased PCNA expression (Figure 4F). Given that ORAI3 controls MiaPaCa2 proliferation, we next investigated if it regulates cell cycle progression in these cells. Flow cytometry analysis revealed that ORAI3 silencing significantly altered cell cycle distribution. More specifically, the fraction of cells in G2/M phase significantly increased in siORAI3-transfected cells compared to siCT-transfected cells. This effect was accompanied by a concomitant decrease in G0/G1-phase population (Figure 4G).

These data suggest that ORAI3 silencing in MiaPaCa2 cells induces proliferative blockade via cell cycle arrest in G2/M phase.

3.6 ORAI3 silencing impairs cell viability and clonogenic survival in MiaPaCa2 cells.

To ensure the effective knockdown of ORAI3 over an extended period of time, cells were retransfected with either siCT or siORAI3 on the 5th day. Interestingly, starting from day 4 post initial siORAI3 transfection, a decrease in cell viability became evident (Figure 5A). We next checked if ORAI3 is important for cell clonogenic

survival. Cells were plated on 6-well plates at a density of 500 cells/well and transfected with siORAI3 or siCT. The next day the medium was changed and cells were left to recover for 10 days. Cell colonies were then photographed and counted. ORAI3 silencing resulted in a significant reduction in clonogenic survival (Figure 5C), again suggesting the prosurvival role of ORAI3 in MiaPaCa2 cells.

3.7 ORAI3 silencing induces mitotic catastrophe followed by caspase-dependent apoptosis *in vitro*.

ORAI3 silencing resulted in significant changes in nuclear morphology. Interestingly, along with an increase in “classical” apoptotic condensed/fragmented nuclei, we also observed many cells with multiple nuclei/micronuclei, the morphological hallmark of mitotic catastrophe (MC) (Figure 5D, 5E & 5F). We therefore next assessed whether ORAI3 silencing induces apoptosis in MiaPaCa2 cells. Cells were transfected with siORAI3 (to ensure the continuous knockdown of ORAI3, cells were transfected with siORAI3 at day 1 and 5) and collected after 10 days. We have confirmed that ORAI3 silencing induces caspase-dependent apoptosis by using TUNEL assay (Figure 5G), and by showing an increase in PARP cleavage (Figure 5H and 5I), which is a crucial mediator of caspase-dependent apoptosis.

Thus, we conclude that siRNA-mediated knockdown of ORAI3 in MiaPaCa2 cells initially results in decreased proliferation and cell cycle arrest (in G2/M phase), and then leads to cell death through mitotic catastrophe and apoptosis.

3.8 ORAI3 silencing inhibits tumor growth and promotes apoptosis *in vivo*.

To test whether ORAI3 silencing could impair tumor growth *in vivo*, we conducted experiments using nude mice bearing MiaPaCa2-derived xenografts. To achieve ORAI3 knockdown in tumors, siORAI3 was injected i.p. on a daily basis. Animals

from control group were injected with siCT. Tumor growth was significantly reduced in siORAI3-treated animals compared to control (Figure 6A & 6B). This impairment of tumor growth correlated with downregulation of ORAI3 mRNA expression in tumors from siORAI3-treated mice (Figure 6C & 6D). Using TUNEL staining on thin tumor sections, we observed an important induction of apoptosis in siORAI3 tumors when compared to siCT treated mouse, which could explain the impairment in tumor growth observed (Figure 6E).

This result suggests that targeting ORAI3 could potentially represent a beneficial strategy in pancreatic cancer treatment.

4. Discussion

In this study, we show that ORAI3 is expressed in human PDAC tumor samples and in several PDAC and HPDE cell lines. Moreover we show that ORAI3 is more expressed in human pancreatic cancer tissue versus paired normal pancreatic tissue, and that ORAI3 gene expression is higher in cancer cell lines compared to a HPDE cell line. These expression patterns indirectly suggest that ORAI3 could have a role in the increased survival capabilities of pancreatic cancer cells. Considering that ORAI3 has been shown to participate to SOCE in several cell types and to be involved in different pathologies such as cancer, we here tested if this protein-forming channel is involved in SOCE in PDAC cells. Interestingly, ORAI3 silencing increased SOCE in PDAC cell lines, while decreasing it in a HPDE cell line. These results suggest that ORAI3 acts as a SOCE repressor in cancer cells, whereas in normal cells ORAI3 could potentially contribute to SOCE. Although these results seemingly contradict previously published data, we can propose a possible explanation. ORAI3 has been shown to mediate SOCE in estrogen receptor positive

breast cancer cells as well as in non small cell lung adenocarcinoma cells [13,15]□. However, along with ORAI1, ORAI3 has been reported to be an important component of the so called store-independent arachidonate-regulated Ca^{2+} (ARC) entry, as well as of a store-independent leukotriene-C4-regulated Ca^{2+} (LRC) entry [10,24]. In addition, the increased expression of ORAI3 in prostate cancer has been demonstrated to promote cell proliferation by increasing ARC-mediated calcium entry. Here we show, that arachidonic acid treatment induces (1) an increase of cytosolic calcium concentration in a pancreatic cancer cell line but not in a normal pancreatic cell line (HPDE) and (2) a decrease of SOCE in pancreatic cancer cells. ARC channels are heteromeric membrane calcium channels formed by the association of ORAI1 and ORAI3 proteins. SOC channels can be either homomeric complexes formed by ORAI1 proteins, or heteromeric complexes made of ORAI1 and ORAI3 proteins. Therefore, an increase in ORAI3 expression would favor the formation of more heteromeric ORAI1/ORAI3 calcium channels (that can be ARC or SOC), while impeding the formation of homomeric ORAI1 calcium channels. If so, ORAI3 silencing would “liberate” ORAI1 from potential heteromeric complexes formation, so that more homomeric ORAI1 complexes can be formed, thus leading to SOCE increase. It has been shown in breast cancer cell lines that ORAI3 participation to the SOCE changes the calcium selectivity of the current [13]. Recently, Yoast and colleague developed this concept by using single, double, and triple gene deletion of native ORAI channels in HEK cells. They demonstrate that by working together, ORAI channels can shape the cytosolic Ca^{2+} signal [25]. In this paper, authors also demonstrate that the incorporation of ORAI3 and ORAI2 with ORAI1 fine-tunes SOC channel activity, a result supporting our observation that SOCE increases after ORAI3 silencing.

Interestingly, in “normal” HPDE cells, ORAI3 seems essential to native SOCE in contrast to cancer cells. Conceptually, these results suggest that in cancer there is a possibility of greater "plasticity" in the molecular organization of SOCE that is not found in normal cells. In other words, ORAI3 could change its “specialization” during malignant transformation, and thus cancer and normal cells could use ORAI3 in different ways and possibly for different purposes.

Beside its role as a protein-forming channel, a non-canonical role of ORAI3 has been described [26]. The authors demonstrated that ORAI1 and ORAI3 proteins could be more important than calcium influx to control cell proliferation (in HEK and Hela cells), and that this process is probably independent of ICRAC and Iarc. To address that question, further investigations with the design of ORAI3 pore mutants and specific cell culture conditions (low extracellular calcium concentration, intracellular calcium chelators) are needed to distinguish canonical (calcium-mediated) and non-canonical (calcium-independent) role(s) of ORAI3 in proliferation and apoptosis.

Furthermore, we have shown that ORAI3 silencing in MiaPaCa2 cancer cells results in decreased proliferation and cell cycle arrest (in G2/M phase). These results strongly suggest that ORAI3 plays a pro-survival and pro-proliferative role in PDAC cells, consistent with previously published data [15,27,28].

After a long siRNA treatment against ORAI3, our data suggest that ORAI3 participates to apoptosis and mitotic catastrophe. Mitotic catastrophe is a cellular process that has been proposed to be onco-suppressive, evasion from mitotic catastrophe thus favoring cancer development [29]. Resistance to cell death and genomic instability (i.e. P53 independency) are also closely linked. The increase in genomic instability allows tumor cells to grow in a stressful environment, but in return

tumor cells are intrinsically more susceptible to mitotic aberrations, and hence, are particularly sensitive to the induction of mitotic catastrophe. Thus, mitotic catastrophe has been proposed in the treatment of PDAC, in mono-therapy or combined therapy, to increase the efficiency of conventional therapies [30,31]. In this context, we demonstrate that *in vivo* silencing of ORAI3 inhibits xenograft tumor growth, while inducing apoptosis, suggesting that ORAI3 could potentially be a useful anticancer therapeutic target.

Acknowledgements

We thank Dr. Ming-Sound Tsao (Ontario Cancer Institute, Toronto, ON, Canada) for the H6C7 cell line. We thank Dr Bruno Serranito (Muséum national d'Histoire naturelle, Paris) for bioinformatics analysis. This work have been supported by INSERM, Ligue Nationale Contre le Cancer, Ministere de l'Education Nationale, Hauts de France, La fondation de France, and I-SITE ULNE that supported C.D. Graphical Abstract was adapted from Servier Medical Art, licensed under a Creative Common Attribution 3.0 Generic License. <http://smart.servier.com/>.

Authors contributions :

K.K and CD designed research studies, performed the experiments, conceived the experimental designs, analyzed the data, and drafted the manuscript. A.K L.M, V.F, N.Z-G, E.L, F.V-A, performed and analysed *in vitro* experiments. R-A.T performed cell cycle analysis. K.K, A.K and A.M performed *in vivo* experiments. L.L and N.P. directed the study, designed research studies, and drafted the manuscript.

Conflict of interest

The authors declare no conflict of interest.

[1] F. Bray, J. Ferlay, I. Soerjomataram, R.L. Siegel, L.A. Torre, A. Jemal, Global

cancer statistics 2018: GLOBOCAN estimates of incidence and mortality worldwide for 36 cancers in 185 countries, *CA Cancer J Clin.* 68 (2018) 394–424. <https://doi.org/10.3322/caac.21492>.

[2] E.S. Christenson, E. Jaffee, N.S. Azad, Current and emerging therapies for patients with advanced pancreatic ductal adenocarcinoma: a bright future, *Lancet Oncol.* 21 (2020) e135–e145. [https://doi.org/10.1016/S1470-2045\(19\)30795-8](https://doi.org/10.1016/S1470-2045(19)30795-8).

[3] S. Zeng, M. Pöttler, B. Lan, R. Grützmann, C. Pilarsky, H. Yang, Chemoresistance in Pancreatic Cancer, *Int J Mol Sci.* 20 (2019). <https://doi.org/10.3390/ijms20184504>.

[4] N. Prevarskaya, R. Skryma, Y. Shuba, Ion Channels in Cancer: Are Cancer Hallmarks Oncochannelopathies?, *Physiol. Rev.* 98 (2018) 559–621. <https://doi.org/10.1152/physrev.00044.2016>.

[5] N. Prevarskaya, R. Skryma, Y. Shuba, Targeting Ca²⁺ transport in cancer: close reality or long perspective?, *Expert Opin. Ther. Targets.* 17 (2013) 225–241. <https://doi.org/10.1517/14728222.2013.741594>.

[6] J.T. Smyth, S.-Y. Hwang, T. Tomita, W.I. DeHaven, J.C. Mercer, J.W. Putney, Activation and regulation of store-operated calcium entry, *J. Cell. Mol. Med.* 14 (2010) 2337–2349. <https://doi.org/10.1111/j.1582-4934.2010.01168.x>.

[7] A.B. Parekh, J.W. Putney, Store-operated calcium channels, *Physiol Rev.* 85 (2005) 757–810. <https://doi.org/10.1152/physrev.00057.2003>.

[8] M. Prakriya, R.S. Lewis, Regulation of CRAC channel activity by recruitment of silent channels to a high open-probability gating mode, *J. Gen. Physiol.* 128 (2006) 373–386. <https://doi.org/10.1085/jgp.200609588>.

[9] J. Roos, P.J. DiGregorio, A.V. Yeromin, K. Ohlsen, M. Lioudyno, S. Zhang, O. Safrina, J.A. Kozak, S.L. Wagner, M.D. Cahalan, G. Veliçelebi, K.A. Stauderman, STIM1, an essential and conserved component of store-operated Ca²⁺ channel function, *J. Cell Biol.* 169 (2005) 435–445. <https://doi.org/10.1083/jcb.200502019>.

[10] T.J. Shuttleworth, Orai3--the “exceptional” Orai?, *J. Physiol. (Lond.)*. 590 (2012) 241–257. <https://doi.org/10.1113/jphysiol.2011.220574>.

[11] S. Bertin, Y. Aoki-Nonaka, P.R. de Jong, L.L. Nohara, H. Xu, S.R. Stanwood, S. Srikanth, J. Lee, K. To, L. Abramson, T. Yu, T. Han, R. Touma, X. Li, J.M. González-Navajas, S. Herdman, M. Corr, G. Fu, H. Dong, Y. Gwack, A. Franco, W.A. Jefferies, E. Raz, The ion channel TRPV1 regulates the activation and proinflammatory properties of CD4⁺ T cells, *Nat. Immunol.* 15 (2014) 1055–1063. <https://doi.org/10.1038/ni.3009>.

[12] M. Trebak, J.W. Putney, ORAI Calcium Channels, *Physiology.* 32 (2017) 332–342. <https://doi.org/10.1152/physiol.00011.2017>.

[13] R.K. Motiani, I.F. Abdullaev, M. Trebak, A novel native store-operated calcium channel encoded by Orai3: selective requirement of Orai3 versus Orai1 in estrogen receptor-positive versus estrogen receptor-negative breast cancer cells, *J. Biol.*

Chem. 285 (2010) 19173–19183. <https://doi.org/10.1074/jbc.M110.102582>.

[14] C. Dubois, F. Vanden Abeele, V. Lehen'kyi, D. Gkika, B. Guarmit, G. Lepage, C. Slomianny, A.S. Borowiec, G. Bidaux, M. Benahmed, Y. Shuba, N. Prevarskaya, Remodeling of channel-forming ORAI proteins determines an oncogenic switch in prostate cancer, *Cancer Cell*. 26 (2014) 19–32. <https://doi.org/10.1016/j.ccr.2014.04.025>.

[15] A.-S. Ay, N. Benzerdjeb, H. Sevestre, A. Ahidouch, H. Ouadid-Ahidouch, Orai3 Constitutes a Native Store-Operated Calcium Entry That Regulates Non Small Cell Lung Adenocarcinoma Cell Proliferation, *PLOS ONE*. 8 (2013) e72889. <https://doi.org/10.1371/journal.pone.0072889>.

[16] I. Bogeski, C. Kummerow, D. Al-Ansary, E.C. Schwarz, R. Koehler, D. Kozai, N. Takahashi, C. Peinelt, D. Griesemer, M. Bozem, Y. Mori, M. Hoth, B.A. Niemeyer, Differential redox regulation of ORAI ion channels: a mechanism to tune cellular calcium signaling, *Sci Signal*. 3 (2010) ra24. <https://doi.org/10.1126/scisignal.2000672>.

[17] K. Kondratska, A. Kondratskyi, M. Yassine, L. Lemonnier, G. Lepage, A. Morabito, R. Skryma, N. Prevarskaya, Orai1 and STIM1 mediate SOCE and contribute to apoptotic resistance of pancreatic adenocarcinoma, *Biochim. Biophys. Acta*. 1843 (2014) 2263–2269. <https://doi.org/10.1016/j.bbamcr.2014.02.012>.

[18] G. Bidaux, D. Gordienko, G. Shapovalov, V. Farfariello, A. Borowiec, O. Iamshanova, L. Lemonnier, M. Gueguinou, R. Guibon, G. Fromont, M. Paillard, Y. Gouriou, C. Chouabe, E. Dewailly, D. Gkika, P. López-Alvarado, J. Carlos Menéndez, L. Hélot, C. Slomianny, N. Prevarskaya, 4TM-TRPM8 channels are new gatekeepers of the ER-mitochondria Ca²⁺ transfer, *Biochimica et Biophysica Acta (BBA) - Molecular Cell Research*. 1865 (2018) 981–994. <https://doi.org/10.1016/j.bbamcr.2018.04.007>.

[19] S. J, A.-C. I, F. E, K. V, L. M, P. T, P. S, R. C, S. S, S. B, T. Jy, W. Dj, H. V, E. K, T. P, C. A, Fiji: an open-source platform for biological-image analysis, *Nature Methods*. 9 (2012). <https://doi.org/10.1038/nmeth.2019>.

[20] S. Davis, P.S. Meltzer, GEOquery: a bridge between the Gene Expression Omnibus (GEO) and BioConductor, *Bioinformatics*. 23 (2007) 1846–1847. <https://doi.org/10.1093/bioinformatics/btm254>.

[21] B. L, H. V, D. So, D. T, P. I, Combined gene expression analysis of whole-tissue and microdissected pancreatic ductal adenocarcinoma identifies genes specifically overexpressed in tumor epithelia, *Hepato-Gastroenterology*. 55 (2008). <https://pubmed.ncbi.nlm.nih.gov/19260470/> (accessed December 2, 2020).

[22] N. Woods, J. Trevino, D. Coppola, S. Chellappan, S. Yang, J. Padmanabhan, Fendiline inhibits proliferation and invasion of pancreatic cancer cells by interfering with ADAM10 activation and β -catenin signaling, *Oncotarget*. 6 (2015) 35931–35948.

[23] H.Y. Khan, G.B. Mpiilla, R. Sexton, S. Viswanadha, K.V. Penmetsa, A. Aboukameel, M. Diab, M. Kamgar, M.N. Al-Hallak, M. Szlaczky, A. Tesfaye, S. Kim,

P.A. Philip, R.M. Mohammad, A.S. Azmi, Calcium Release-Activated Calcium (CRAC) Channel Inhibition Suppresses Pancreatic Ductal Adenocarcinoma Cell Proliferation and Patient-Derived Tumor Growth, *Cancers (Basel)*. 12 (2020). <https://doi.org/10.3390/cancers12030750>.

[24] J.C. González-Cobos, X. Zhang, W. Zhang, B. Ruhle, R.K. Motiani, R. Schindl, M. Muik, A.M. Spinelli, J.M. Bisailon, A.V. Shinde, M. Fahrner, H.A. Singer, K. Matrougui, M. Barroso, C. Romanin, M. Trebak, Store-independent Orai1/3 channels activated by intracrine leukotriene C4: role in neointimal hyperplasia, *Circ. Res.* 112 (2013) 1013–1025. <https://doi.org/10.1161/CIRCRESAHA.111.300220>.

[25] R.E. Yoast, S.M. Emrich, X. Zhang, P. Xin, M.T. Johnson, A.J. Fike, V. Walter, N. Hempel, D.I. Yule, J. Sneyd, D.L. Gill, M. Trebak, The native ORAI channel trio underlies the diversity of Ca²⁺ signaling events, *Nature Communications*. 11 (2020) 2444. <https://doi.org/10.1038/s41467-020-16232-6>.

[26] A.-S. Borowiec, G. Bidaux, R. Tacine, P. Dubar, N. Pigat, P. Delcourt, O. Mignen, T. Capiod, Are Orai1 and Orai3 channels more important than calcium influx for cell proliferation?, *Biochim. Biophys. Acta.* 1843 (2014) 464–472. <https://doi.org/10.1016/j.bbamcr.2013.11.023>.

[27] M. Faouzi, F. Hague, M. Potier, A. Ahidouch, H. Sevestre, H. Ouadid-Ahidouch, Down-regulation of Orai3 arrests cell-cycle progression and induces apoptosis in breast cancer cells but not in normal breast epithelial cells, *J. Cell. Physiol.* 226 (2011) 542–551. <https://doi.org/10.1002/jcp.22363>.

[28] M. Faouzi, P. Kischel, F. Hague, A. Ahidouch, N. Benzerdjeb, H. Sevestre, R. Penner, H. Ouadid-Ahidouch, ORAI3 silencing alters cell proliferation and cell cycle progression via c-myc pathway in breast cancer cells, *Biochimica et Biophysica Acta (BBA) - Molecular Cell Research*. 1833 (2013) 752–760. <https://doi.org/10.1016/j.bbamcr.2012.12.009>.

[29] T.V. Denisenko, I.V. Sorokina, V. Gogvadze, B. Zhivotovsky, Mitotic catastrophe and cancer drug resistance: A link that must to be broken, *Drug Resist Updat.* 24 (2016) 1–12. <https://doi.org/10.1016/j.drug.2015.11.002>.

[30] A. Mathison, A. Salmonson, M. Missfeldt, J. Bintz, M. Williams, S. Kossak, A. Nair, T.M. de Assuncao, T. Christensen, N. Buttar, J. Iovanna, R. Huebert, G. Lomberk, Combined AURKA and H3K9 Methyltransferase Targeting Inhibits Cell Growth By Inducing Mitotic Catastrophe, *Mol Cancer Res.* 15 (2017) 984–997. <https://doi.org/10.1158/1541-7786.MCR-17-0063>.

[31] R. Florio, S. Veschi, V. di Giacomo, S. Pagotto, S. Carradori, F. Verginelli, R. Cirilli, A. Casulli, A. Grassadonia, N. Tinari, A. Cataldi, R. Amoroso, A. Cama, L. De Lellis, The Benzimidazole-Based Anthelmintic Parbendazole: A Repurposed Drug Candidate That Synergizes with Gemcitabine in Pancreatic Cancer, *Cancers (Basel)*. 11 (2019). <https://doi.org/10.3390/cancers11122042>.

Titles and figures legends

Figure 1. ORAI3 is overexpressed in cancer PDAC human tumors and PDAC cell lines. (A) ORAI1 and ORAI3 protein expression in normal (N) and tumor (T) pancreatic adenocarcinoma (B) ORAI3 gene expression levels relative to GAPDH in normal HPDE (H6C7) and PDAC cell lines (Capan1, ASPC1, Panc1, MiaPaCa2 and BxPC3). Data presented as means \pm S.D. N=3.

Figure 2. ORAI3 silencing increases SOCE in PDAC but not in normal pancreatic cells. Representative calcium imaging measurements of TG-activated SOCE as indicated by $[Ca^{2+}]_c$ elevation and normalized calcium entry quantification, 48hr after treatment with control (siCT) or siORAI3 for HPDE (H6C7) (A,B), BxPC3 (C,D), AsPC1 (E,F), MiaPaCa2 (G,H), Capan1 (I,J) and Panc1 (K,L) cell lines. *p < 0.05. Error bars represent means \pm SEM. n=30-100 cells. N=3

Figure 3. ORAI3 silencing increases capacitative calcium entry in PDAC cells. Representative calcium imaging measurements of calcium switch-activated (0mM to 10mM extracellular) SOCE as indicated by $[Ca^{2+}]_c$ elevation and normalized calcium entry quantification, 48hr after treatment with control (siCT) or siORAI3 in Panc1 (A) Capan1 (B) and MiaPaCa2 (C) cell lines. (D) Representative calcium imaging measurements of Arachidonic-Acid-induced calcium entry in MiaPaCa2 and normal HPDE cells. (E) Representative cytosolic calcium imaging measurements following ER calcium depletion (Thapsigargin) after a 30 min pretreatment with AA (8 μ M) or DMSO (CT). Data are represented as means \pm S.E.M. n=30-100 cells. *p < 0.05. (N=3).

Figure 4. ORAI3 silencing decreases cell proliferation via cell cycle arrest in G2/M-phase and affects cell morphology. Proliferation quantification relative to untransfected cell (CT) obtained by MTS assay after 48h preceded by a 48h

treatment with siCT or siORAI3 (40nM) for Panc1 (A), Capan1 (B), and MiaPaCa2 (C). (D) Light microscopy photographs of MiaPaCa2, BxPC3 and Panc1 cell lines transfected either with siCT or siORAI3 showing a significant increase in cell size, and an unusual cell shape as well as cell flattening as indicated by blue arrows. (E) Manual cell counting normalized to siCT treated cells. (F) Representative Western blots of PCNA protein levels for siCT and siORAI3 treated MiaPaCa2 cells. Quantifications presented are mean of 3 independent experiments. Ratio is relative to siCT intensity /actine intensity =1. (G) Representative distribution (%) of cells in Sub G1-, G0/G1-, S-, and G2/M-phases for siCT and siORAI3 after 96h (48h siRNA treatment and 48h proliferation). *p < 0.05. Data are presented as means±S.E.M. and means±S.D for G. (N=3).

Figure 5. ORAI3 silencing impairs MiaPaCa2 cell viability, clonogenic survival, and induces mitotic catastrophe leading to apoptosis. (A) Cell viability assessed by MTS assay after 4, 7 and 10 days of siRNA treatment. (B) Representative pictures of dishes after clonogenic assay stained with crystal violet and seeded with untreated cells (CT) or cells treated with siCT or siORAI3 (C) Manual quantifications of colonies. (D) Upper panel, nuclear morphology after HOECHST staining of MiaPaCa2 cells 10 days after transfection with siCT or siORAI3. Lower panel, cells undergoing apoptosis (white arrows) or mitotic catastrophe (red arrows) are presented. (E) Percentage of multinucleated cells (undergoing mitotic catastrophe) in siCT- or siORAI3 treated cells. (F) Quantification of apoptosis in siCT- and siORAI3-treated cells. (G) Representative confocal images of TUNEL stained MiaPaCa2 cells treated with siCT or siORAI3 for 10 days. (H) Representative Western blots of PARP and cleaved PARP proteins in CT and siORAI3 MiaPaCa2 treated cells. (I) Protein

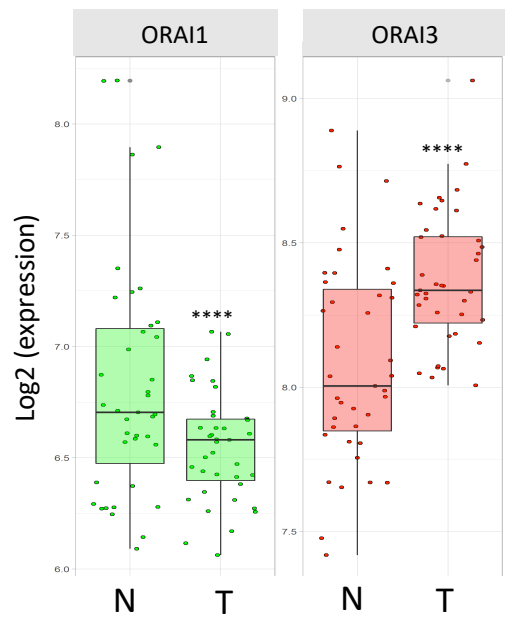
quantification of (H) representing the mean of 3 experiments. One sample t-test and Wilcoxon. Data are represented as means±S.E.M. *p < 0.05. (N=3).

Figure 6. ORAI3 silencing reduces MiaPaCa2 xenograft tumor growth via apoptosis induction. (A) Tumor growth curves for both siCT- and siORAI3-treated mice. (B) Weight of excised tumors (means±S.D.). (C) representative RT-PCR gel showing ORAI3 and actin mRNA levels in xenografted tumors from mice treated with siCT (n=5) or siORAI3 (n=5). (D) Relative ORAI3 gene expression quantification from (C). (E) Representative images of MiaPaCa2 xenograft tumor sections after 21 days of siCT or siORAI3 treatment. Data are represented as means±S.E.M. *p < 0.05.

Figure S1. Normalized TG-calcium induced quantification and Knockdown efficiency of ORAI3 in HPDE and PDAC cell lines. (A-F) ER calcium release induced by Thapsigargin after siORAI3 normalized to siCT for HPDE (A) BxPC3 (B), AsPC1 (C), MiaPaCa2 (D), Capan1 (E) and Panc1 (F) **(G-K)** qRT-PCR detection of ORAI3 gene expression 48h after transfection with siCT or siORAI3 in HPDE (G) BxPC3 (H), AsPC1 (I), MiaPaCa2 (J), and Capan1 (K) cell lines. Data are presented as means±S.E.M. *p < 0.05. (N=3)

Figure S2. Synta66 decreases MiaPaCa2 cells proliferation but does not increase ORAI3 mediated proliferation defect. (A) Proliferation quantification relative to control cell (CT) obtained by MTS assay after a 48h treatment with synta66 (5µM) **(B)** Proliferation quantification relative to control cell (CT) obtained by MTS assay after a 48h treatment with synta66 (5µM) preceded by a 48h treatment with siCT or siORAI3 (40nM) of MiaPaCa2 cells.

A



B

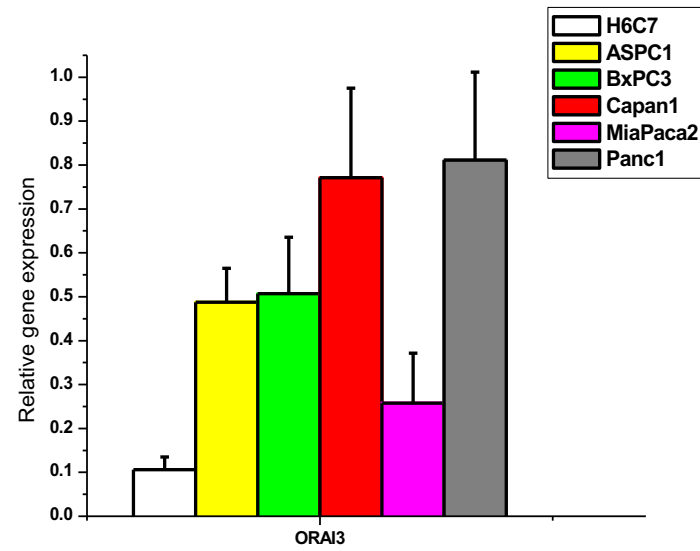


Figure 1

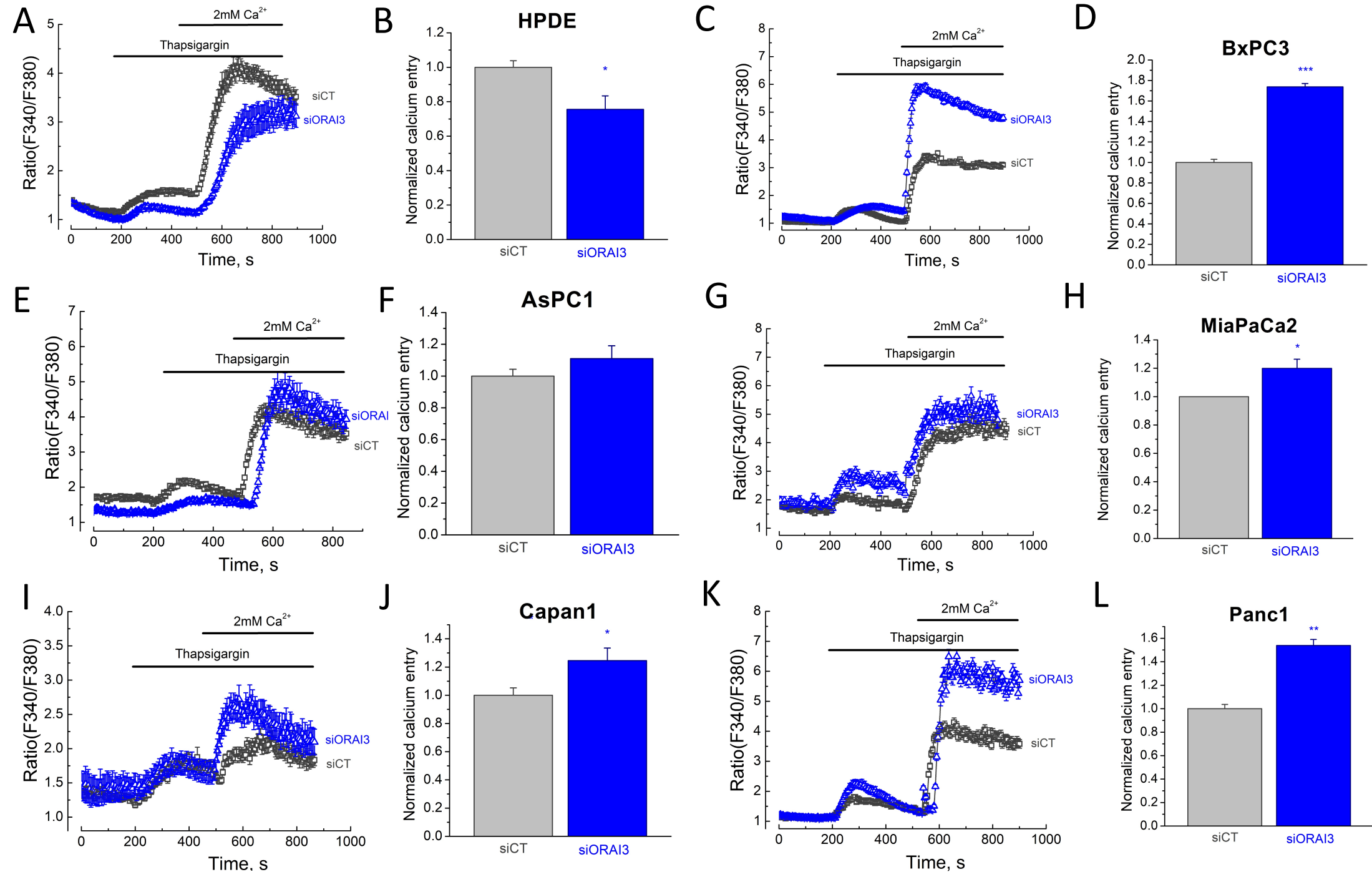


Figure 2

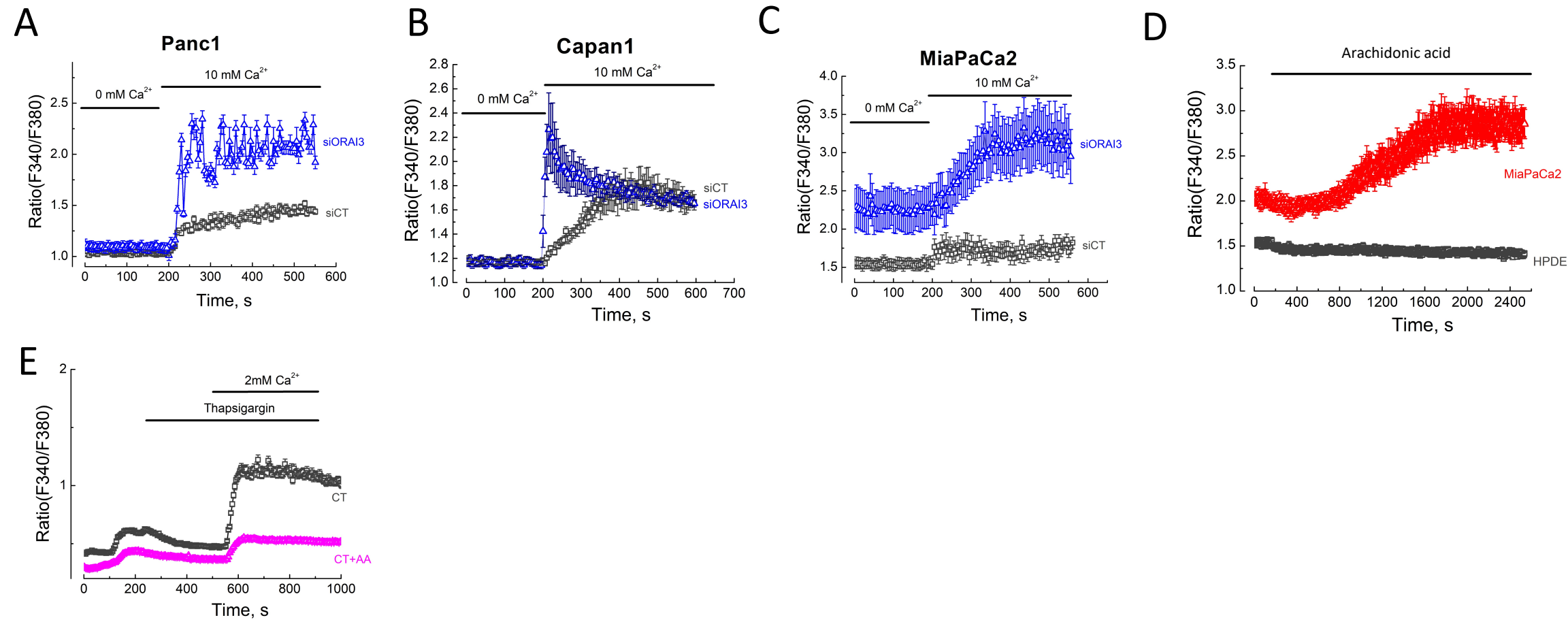


Figure 3

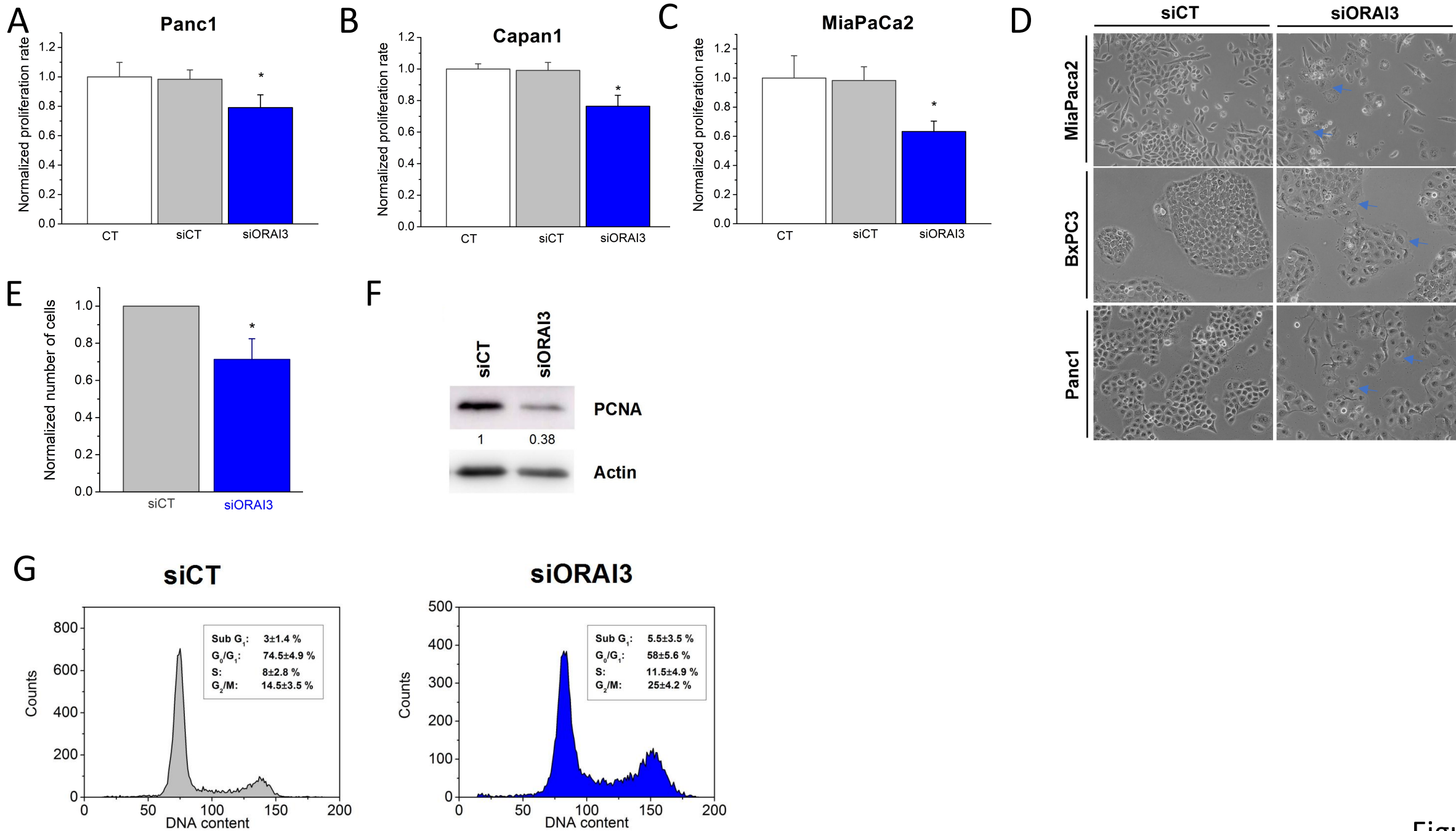


Figure 4

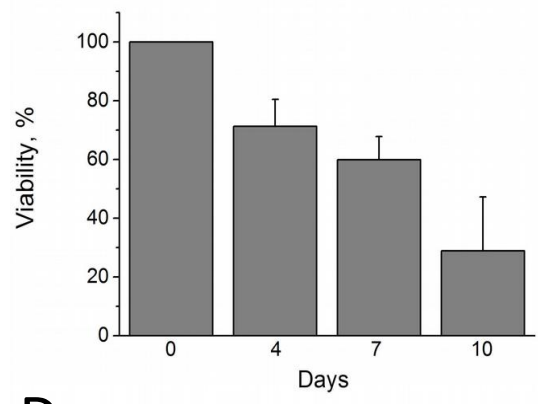
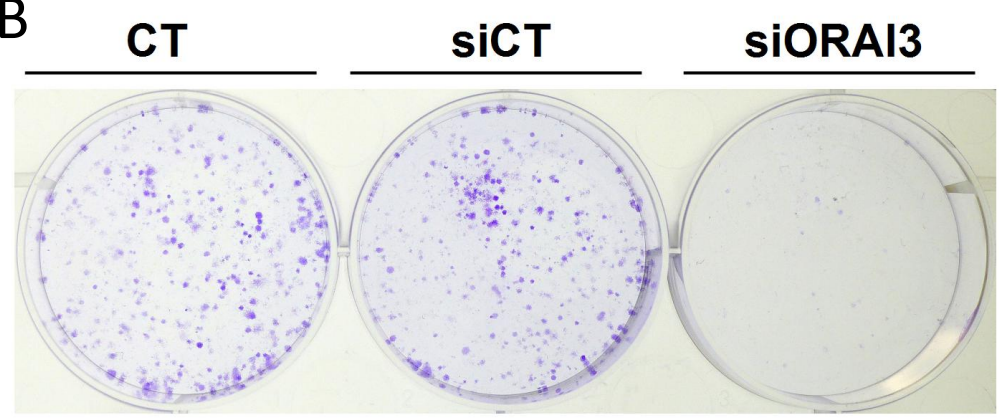
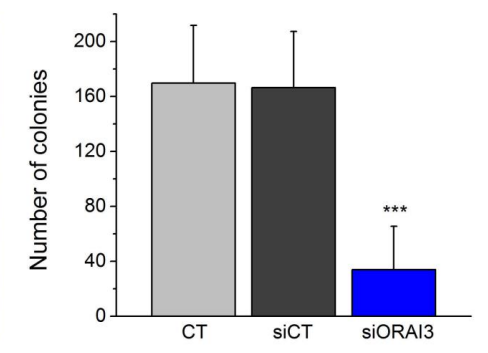
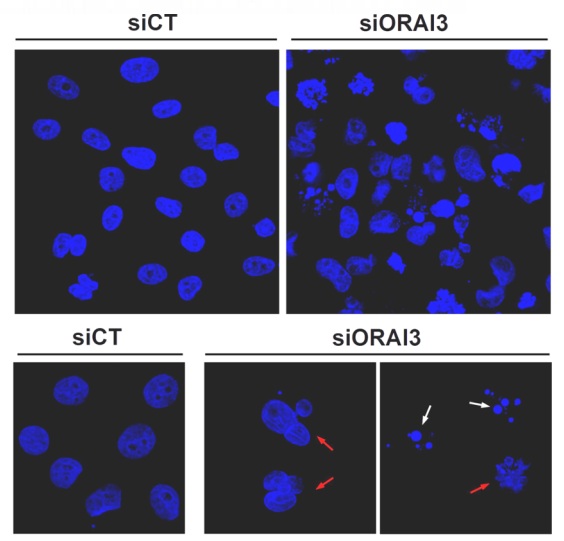
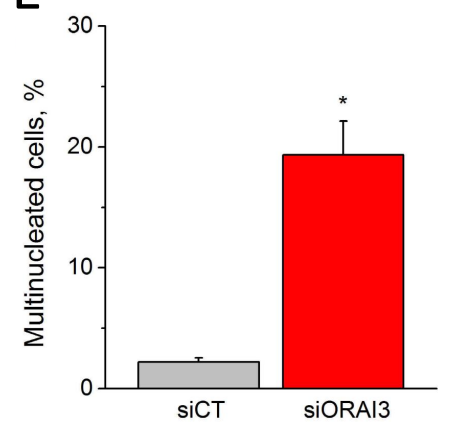
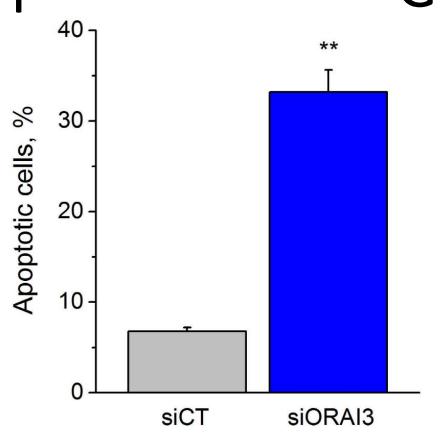
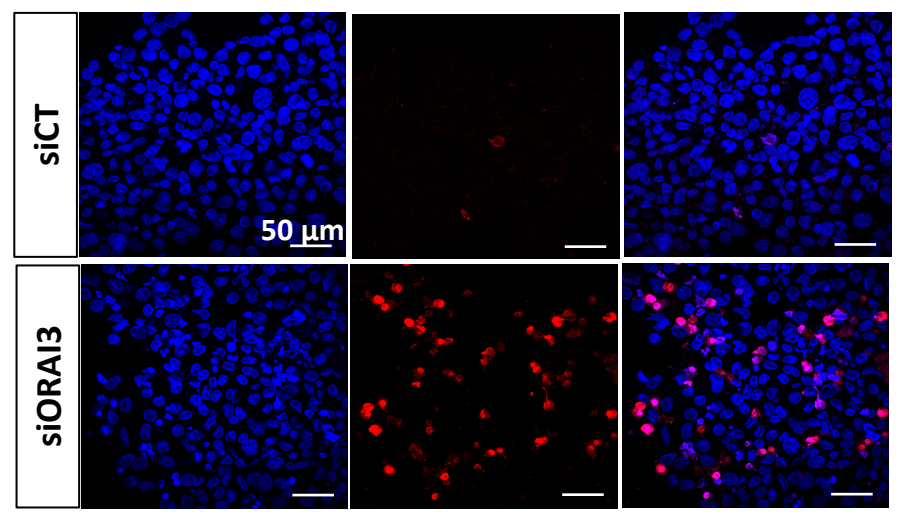
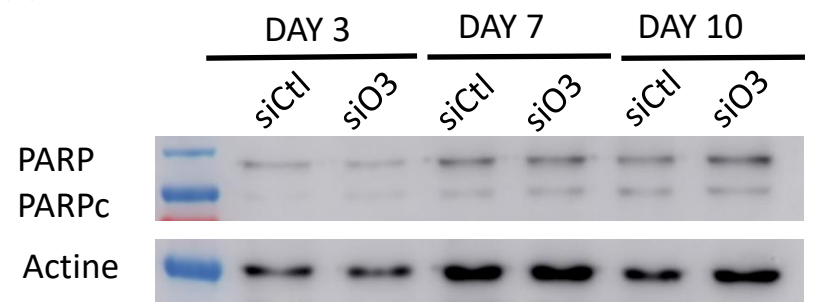
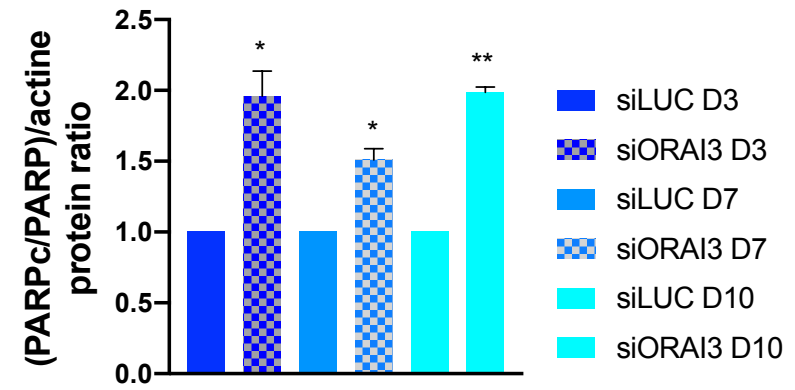
A**B****C****D****E****F****G****H****I**

Figure 5

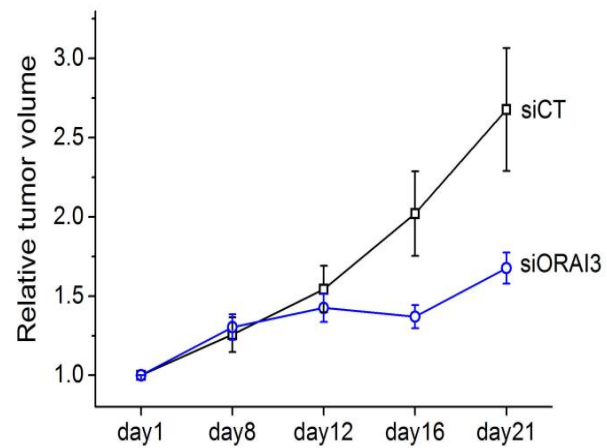
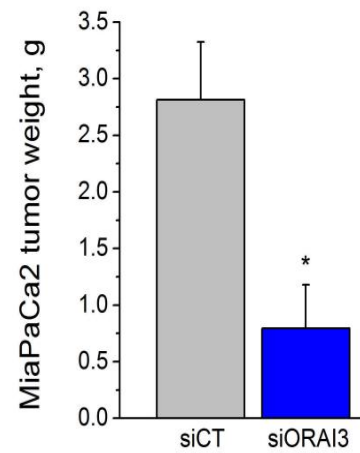
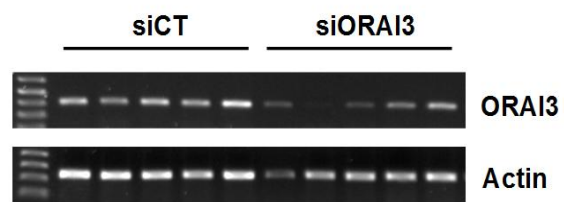
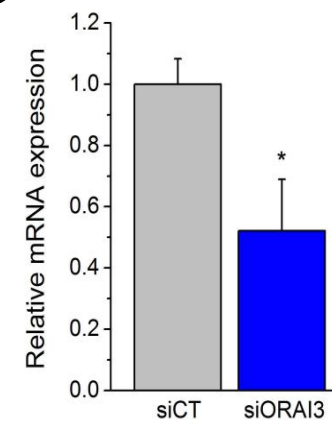
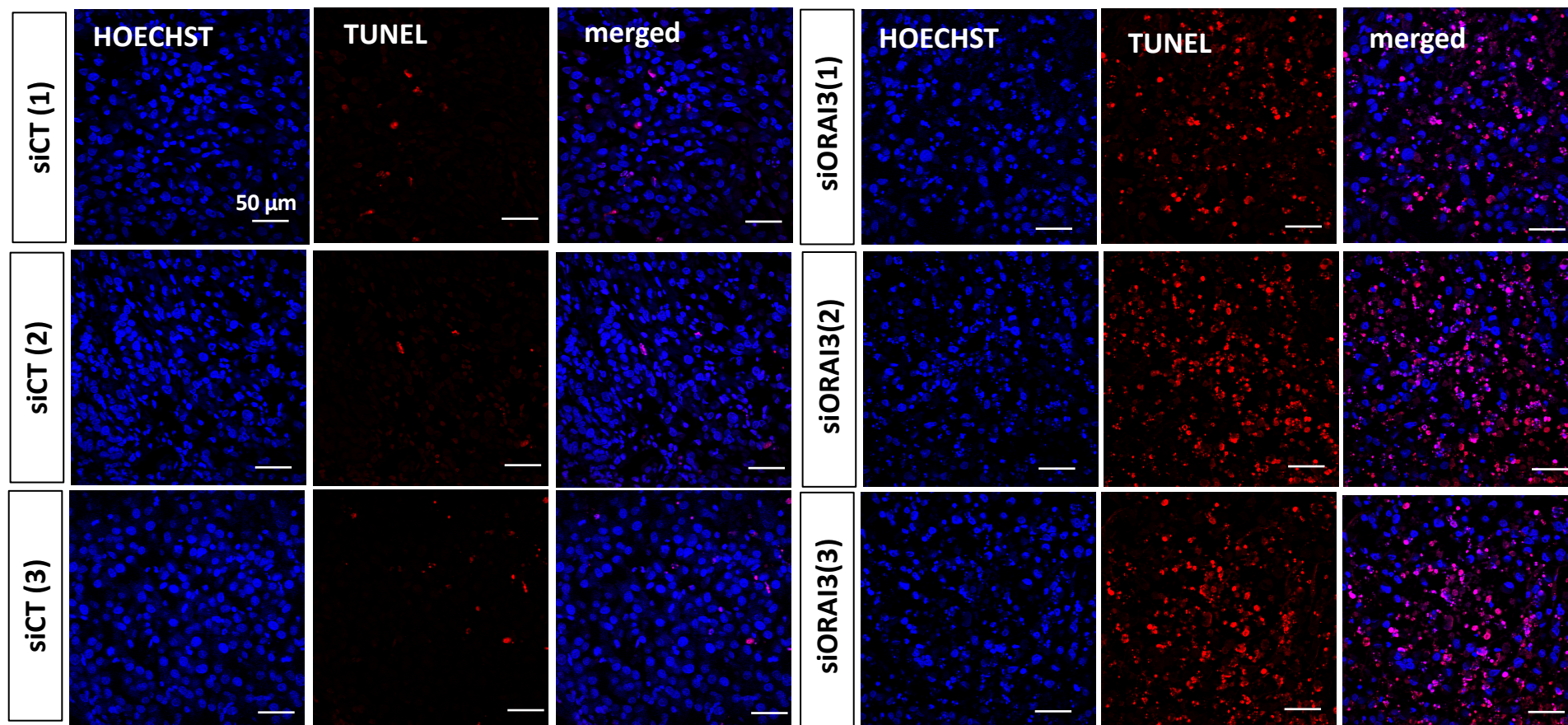
A**B****C****D****E**

Figure 6